

ANALYSIS OF CONTAMINANT TRANSPORT UNDER WIND CONDITIONS ON THE SURFACE OF A SHALLOW LAKE

Laura C. Oporto^{a,b}, Derlis A. Ramírez^a, Jhabriel D. Varela^c and Christian E. Schaerer^{b,d}

^a*Facultad de Ciencias Químicas, Universidad Nacional de Asunción, San Lorenzo, Central, Paraguay,
lauri_oporto@hotmail.es, derandres_ra3@hotmail.com*

^b*Centro de Investigación en Matemática, Asunción, Paraguay*

^c*Universidad Paraguayo Alemana, San Lorenzo, Central, Paraguay, jhabriel@upa.edu.py*

^d*Facultad Politécnica, Universidad Nacional de Asunción, San Lorenzo, Central, Paraguay,
cschaer@pol.una.py*

Keywords: Pollution, Navier-Stokes equations, Finite Volume Method, OpenFOAM.

Abstract. The increasing industrial activities near several lakes in Paraguay have been the main reason for its pollution and, therefore, there is an urgency to find solutions to environmental problems caused. In this paper, contaminant transport, represented by a non-reactive passive scalar transport, is analysed under fluctuating wind conditions. Flow velocities obtained from the two-dimensional (2D) Navier-Stokes equations are used to calculate contaminant concentrations along the considered geometry, which is the surface of the Lake Ypacarai, in Paraguay. The equations are discretized by finite volume method and solved with OpenFOAM(R). Field data measurements of total phosphorus are used to contrast the numerical results. This paper evaluates different pollution scenarios of the Lake Ypacarai varying the direction of the wind, and the numerical results present a great similarity between the simulated results and field measurements, describing qualitatively the behaviour of the considered lake.

1 INTRODUCTION

Worldwide, lakes have played an important role in the development of industries, tourism and agriculture of its surrounding areas. However, increasing human activity and lack of management of this water bodies has worsened their ecological states. Therefore, the increment of polluted lakes represents a challenge for engineers, as they have to be able to provide clean fresh water in great amounts (Tsanis et al., 2006).

One of the factors that has a big impact on the hydrodynamic properties of lakes is the geometry, because changes within the basin produces velocity variations which may lead to advective zones, where velocity fluctuates, as well as dead zones, with very low velocities. Furthermore, the inflows of the lakes can influence the circulation at the entry when the volume of the inlets are considerable big compared to the basin volume (Tsanis et al., 2006). Finally, wind stress is a crucial driving force in lakes (Chao et al., 2008), particularly in shallow lakes, where the flow is primarily induced by wind (Józsa, 2004). The wind shear stress over water produces surface waves, which promote pollutant transport along the lake (Wu et al., 2010). Water waves generated by soft winds also promotes chlorophyll and cyanobacteria growth (Facetti, 2007).

Numerical simulations support field measurements and observations of lakes conditions and contaminant transport processes. In fact, mathematical models provide information regarding the hydrodynamic conditions of the lake that are often required for water quality studies (Tsanis et al., 2006).

In addition, this work presents an analysis of contaminant transport under different wind directions on the surface of the Lake Ypacarai, in Paraguay, due to its high social impact and necessity to improve its environmental condition. Field measurements from the Multidisciplinary Technology Research Center (CEMIT) support the simulated results. Although there are several studies on the effect of wind on lakes, none of them were ever applied to evaluate the Lake Ypacarai. Therefore, through this work we want to provide a tool to locate the areas of higher contamination, which is necessary in the decision-making process.

The outline of this paper is as follows. First, a brief description of the equations and boundary conditions are presented. In Sec. 3, the study area and numerical solution is explained. Numerical results are presented in Sec. 4 and conclusions are summarized in Sec. 5.

2 MODEL DESCRIPTION

2.1 Governing Equations

The Navier-Stokes are adopted as the governing equations (Griebel et al., 1997). They are a set of non-linear partial differential equations, derived from conservation of mass and momentum. For an incompressible and viscous fluid of constant density, the two-dimensional (2D) Navier-Stokes equations are written as follows:

$$\begin{aligned}\rho(\partial_t \mathbf{u} + \mathbf{u} \cdot \nabla \mathbf{u}) &= \mu \nabla^2 \mathbf{u} - \nabla p + \mathbf{f}, \\ \nabla \cdot \mathbf{u} &= 0.\end{aligned}\tag{1}$$

where t is the time, $\mathbf{u} \in \mathbb{R}^2$ is the velocity defined as $\mathbf{u} = (u_1, u_2)^T$, the operator ∇ is defined as $\nabla := (\partial_x, \partial_y)^T$, p is the pressure, μ is the dynamic viscosity, ρ is the density and \mathbf{f} is the source term which represents external forces on the fluid. In this work the turbulence is not included.

The wind shear stresses at the surface are denoted by (Chao et al., 2008; Tsanis et al., 2006):

$$\begin{aligned}\tau_{wx} &= \rho_a C_d u_w \sqrt{u_w^2 + v_w^2}, \\ \tau_{wy} &= \rho_a C_d v_w \sqrt{u_w^2 + v_w^2}.\end{aligned}\quad (2)$$

where τ_{wx} and τ_{wy} are the wind stresses at the direction x and y , respectively; $\mathbf{w} = (u_w, v_w)^T$ is the wind velocity at 10 m of elevation above the still water surface, u_w and v_w are the wind velocity components in x and y , respectively; ρ_a is the air density and C_d is the drag coefficient, which may vary with the wind speed, but usually ranges in the order of 10^{-3} (Chao et al., 2008). The drag coefficient depends on the type of water body considered, and there are different models to calculate its value, such as the formulas proposed by Wu (1980) and Eid (1981). However, for simplicity, C_d is considered to be constant and equal to $1 \cdot 10^{-3}$. The stresses at x and y direction are computed using Eq. (2) and included in Eq. (1) in the source term as the tensor divergence.

In this work, the contaminant is represented by a non reactive scalar, present in a very small amount so that does not produce a dynamic effect in the fluid movement. The 2D mass transport equation is used in order to model contaminant transport:

$$\partial_t c + \mathbf{u} \cdot \nabla c = D \nabla^2 c + f_c. \quad (3)$$

where $c(x, y, t)$ is the concentration of the contaminant and D its diffusivity, a possible chemical reaction is denoted by f_c , although in this work is omitted.

2.2 Boundary conditions

The boundary of the lake $\partial\Omega$ is divided as $\partial\Omega = \partial\Omega_t \cup \partial\Omega_D$ where $\partial\Omega_t$ is the part of the boundary associated to the tributaries and $\partial\Omega_D$ the rest of the boundary. In the contour of the lake, except the tributaries, no-slip boundary condition are considered:

$$\mathbf{u} = \mathbf{u}_{\text{wall}} = 0 \quad \forall (x, y) \in \partial\Omega_D. \quad (4)$$

Outflow boundary condition is imposed at one of the streams, and stream velocities are used as Dirichlet boundary condition at the other two main inflows:

$$\partial_n \mathbf{u} = 0, \quad \forall (x, y) \in \partial\Omega_t \text{ (outflow)} \quad \mathbf{u} = u_{\text{streams}}, \quad \forall (x, y) \in \partial\Omega_t \text{ (inflow)}. \quad (5)$$

with n as the normal direction. The wind shear stress is applied at the internal region of the mesh, not at the boundaries.

3 MODEL APPLICATION

3.1 Study area and parameter values

The equations are discretized by the Finite Volume Method (FVM) and solved at the surface of the Lake Ypacarai. Contour variation due to mass accumulation is beyond the scope of this work. The Lake Ypacarai has an approximate area of 60 km², an average water volume of 38.000.000 m³ and average depth of 2.3 m (Ruíz, 2012). The main inflows are the Yukyry and Pirayu streams, with average annual rate of 0.26 and $0.51 \text{ m} \cdot \text{s}^{-1}$, respectively (Amarilla Pavón, 2014) and the outflow is the Salado river with an average annual rate of $2.6 \text{ m} \cdot \text{s}^{-1}$ (SEAM, 2015). The geometry of the lake is shown in Fig. 1, where the subscripts 1, 2 and 3 ($\partial\Omega_1$, $\partial\Omega_2$ and $\partial\Omega_3$), indicate the Salado river, and the Pirayu and Yukyry streams, respectively.

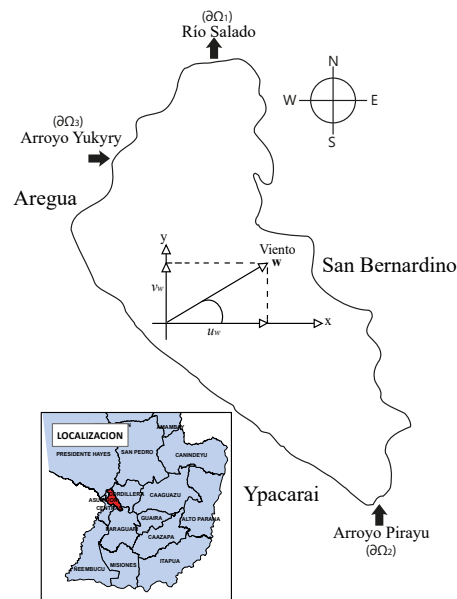


Figure 1: Surface of Lake Ypacarai. $\partial\Omega_1$ is the outflow and $\partial\Omega_2, \partial\Omega_3$ are the inflows.

Wind velocity varies according to annual data from the National Directorate of Civil Aviation (DINAC), where the wind data shows a predominance of Southsoutheast (SSE) and Eastnorth-east (ENE) winds. Wind rose for 2015 is shown in Fig. 2a, where North is 0° . Only Northeast (45°), Southeast (135°), Southwest (225°), and Northwest (315°) winds are considered. Constant wind speed of $15 \text{ km} \cdot \text{h}^{-1}$ is used.

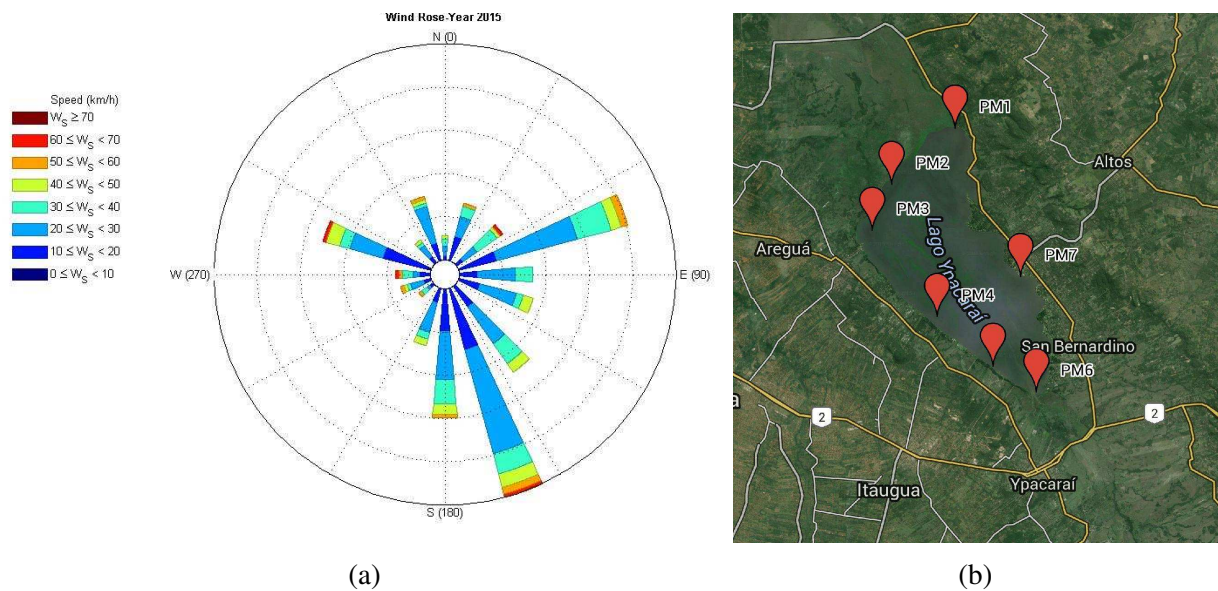


Figure 2: (a) Wind rose, year 2015. (b) Measurement points. CEMIT, 2015.

Contamination results are compared to total phosphorus measurements from the technical report of the fourth monitoring campaign in the lake (CEMIT, 2015), which is available for the general public. These values were obtained by sampling of surface water, based on the standard methods for the examination of water and wastewater (American Public Health Association et al., 1981). The contaminant is introduced at the Yukyry and Pirayu streams simultaneously, with concentrations of 0.08 and $0.101 \text{ mg} \cdot \text{L}^{-1}$, respectively, according to the technical report. The results are compared at the same measurement points presented in the technical report, showed in Fig. 2b. Table 1 shows the references for the measurement points.

Reference	Measurement points
PM1	Salado river
PM2	Yukyry stream
PM3	Aregua beach
PM4	Center of the lake
PM5	Pirayu stream (mouth)
PM6	Pirayu stream
PM7	Club Nautico (San Bernardino)

Table 1: In situ measurement points references

The constant values considered are presented in Table 2

Parameter	Symbol	Value	Measure unit
Water density	ρ	1.000	$\text{kg} \cdot \text{m}^{-3}$
Water dynamic viscosity	μ	$8.937 \cdot 10^{-4}$	$\text{kg} \cdot \text{m}^{-1} \cdot \text{s}^{-1}$
Drag coefficient	C_d	$1 \cdot 10^{-3}$	-
Air density	ρ_a	1.29	$\text{kg} \cdot \text{m}^{-3}$
Wind speed	w	15	$\text{km} \cdot \text{h}^{-1}$
Diffusion coefficient	D	$0.89 \cdot 10^{-9}$	$\text{m}^2 \cdot \text{s}^{-1}$
Time step	Δt	2	s
Initial time	t_0	0	s
End time	t	200.000	s
Parameter	Symbol	Tolerance	
Wind	h	$1 \cdot 10^{-6}$	
Pressure	p	$1 \cdot 10^{-6}$	
Scalar	T	$1 \cdot 10^{-7}$	
Velocity	U	$1 \cdot 10^{-5}$	

Table 2: Constants used in the simulation

3.2 Solver description

The mesh was generated in three steps. First, the lake contour data stored in ArcGIS, a Geographic Information System (GIS), which consists of a set of applications for capturing, editing, analysis, processing, design, publishing and printing of geographic information. Then, it was exported to Autocad[®], where the (x,y) points were manually exported to GMSH, which allows

the user to obtain a mesh with triangular elements. Finally, the mesh in .msh format is transformed into OpenFOAM® readable format with *gmshToFoam* tool. A mesh with 4498 points, 4292 cells and 15124 faces, where 6336 of them are internal faces, and the others are boundary faces was obtained (for further details on the mesh description see [OpenFOAM \(2011\)](#)). The *icoFoam* solver for incompressible laminar flow of Newtonian fluids is used. In order to obtain the solution, the PISO (Pressure Implicit with Splitting of Operator) algorithm with modifications is implemented (Fig. 3).

In this algorithm, the resolution of the system is performed by splitting the operations, in the solution of discretised equations, in predictor and corrective steps. For each time-step, results are approximations of the exact solution, with an accuracy that depends on the number of operation-splittings considered ([Issa, 1986](#)). We consider one predictor and two corrective steps. Two modifications were made in order to solve the system:

1. First modification: add the wind effect to the solver as the source term.
2. Second modification: add the transport equation to obtain the pollutant concentration. It is added after the PISO loop in the solver.

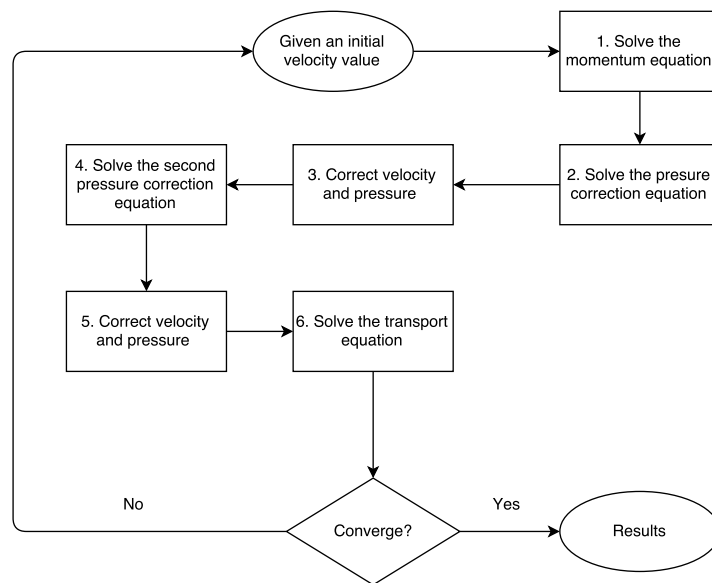


Figure 3: PISO algorithm

4 SIMULATION RESULTS

Contaminant results are presented in absence and presence of wind. Wind speed of $15\text{km} \cdot \text{h}^{-1}$ and wind directions mentioned in Sec. 3.1 are considered and a simulation time of 56h (2.3 days) was adopted.

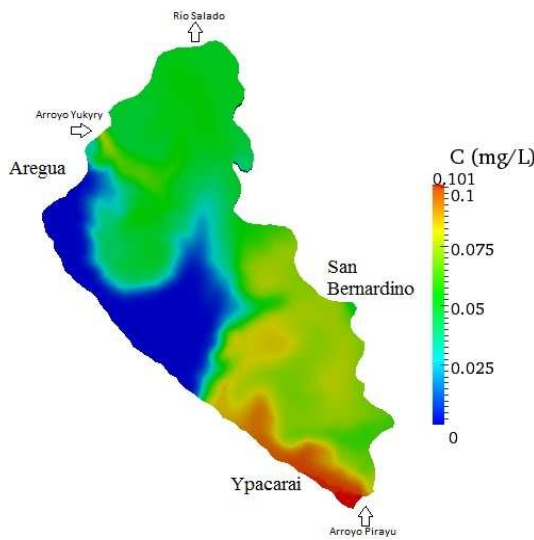


Figure 4: Absence of wind

Figure 4 shows that when a contaminant is introduced through the tributaries and under no-wind conditions, Aregua and the center of the lake are less affected. In addition, Ypacarai, San Bernardino and the Salado river surroundings are more polluted.

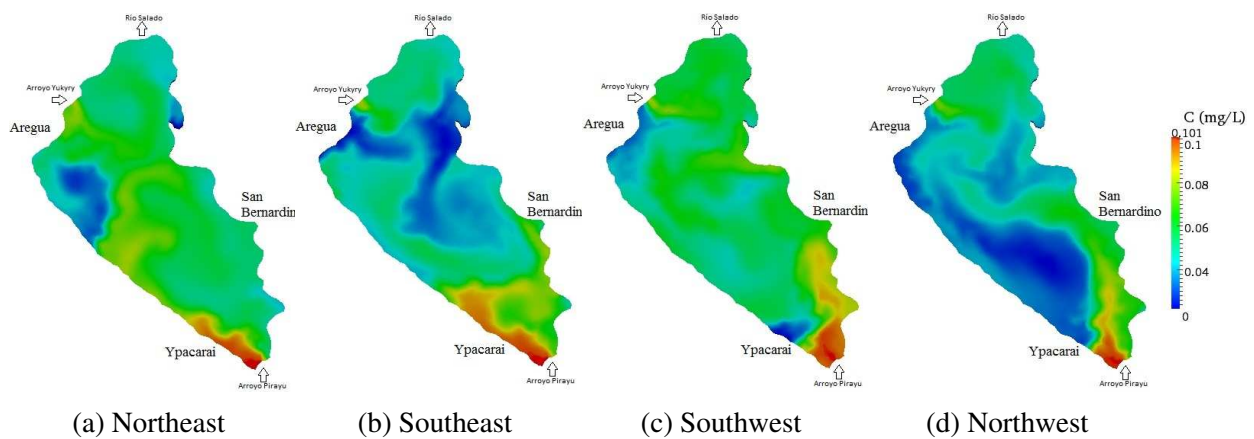


Figure 5: (b) Results for wind-conditions

Figure 5 shows that for Northwest winds (Fig. 5d), Aregua and Ypacarai are less affected than the other case studies. However, for Southeast and Southwest (Fig. 5c) winds (Fig. 5b), this city shows a very low concentration near the Yukyry stream, due to the flow pattern under those wind conditions. Furthermore, Ypacarai is more polluted under Northeast (Fig. 5a) and Southeast (Fig. 5b) and Northwest winds (Fig. 5d) do not have an important impact in this city. Finally, San Bernardino city is more polluted under Southeast (Fig. 5b) and Northwest (Fig. 5d) winds.

Considering that there are no previous computational works on this lake, and the fact that the sampling conditions are not specified, we only perform a qualitative analysis of the results. However, in an attempt to see if our results approach the real measurement data and if the study is on the right path, the percent relative error for each measurement point (Fig. 2b) and each case study were calculated.

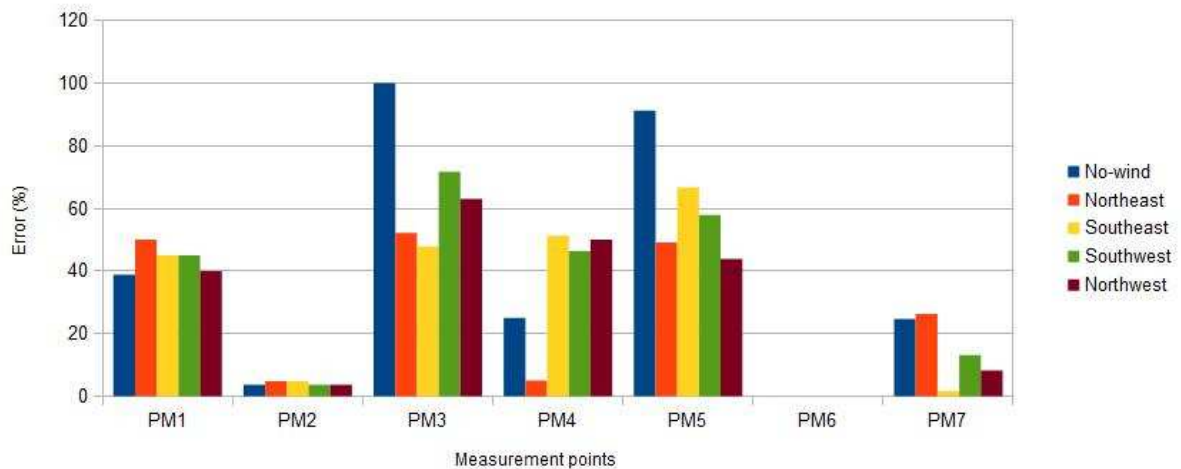


Figure 6: Error values at each measurement point

Figure 6 shows errors values. It shows that Southeast and Northwest winds have the lower errors for most of the measurement points. Error values for the Pirayu stream (PM6) are zero because the same value was used as initial value for the contaminant concentration at that point.

5 SUMMARY AND CONCLUSIONS

Wind direction noticeably affect the contaminant transport, introduced by the tributaries. Furthermore, the study cases show that in general, Ypacarai and Aregua have high concentration of this contaminant in most of the cases, which implies that they are more likely to be polluted.

Comparison between results and data of the fourth monitoring campaign in the lake, shows similarity, demonstrating that these results may qualitatively predict the behaviour of the system and it would be possible to simulate the actual condition of the lake when other factors that affect the dynamics of the lake are considered. In Figure 6, it was noted that the Southeast and Northwest winds have lower errors, which is consistent with the real data.

We consider that our results are good, in the sense that we are looking for qualitative results. This is because no previous experience, neither from simulations nor laboratory, is available for this lake. In addition, the measurement data report does not specify the weather conditions at the moment of the sampling. Therefore, the direct qualitative correlation between the simulation and the sampling data is difficult to establish.

Finally, we consider that it was possible to simulate qualitatively the lake pollution and thus, to provide a basis for future works and to contribute to decision-making process to improve the environmental condition of the lake.

6 ACKNOWLEDGEMENTS

C.E.S. acknowledges the support of PRONII-CONACYT. L.O. thanks the support of CIMA and project 14 - INV - 186 - CONACyT - Paraguay. To CEMIT and DINAC for the measurement data.

REFERENCES

- Amarilla Pavón M.D. Determinación de la carga contaminante del arroyo Yukyry, afluente del Lago Ypacarai. 2014.
- American Public Health Association, Association A.W.W., et al. *Standard methods for the examination of water and wastewater: selected analytical methods approved and cited by the United States Environmental Protection Agency*. American Public Health Association, 1981.
- CEMIT. Monitoreo de calidad de agua por campañas de muestreo en el Lago Ypacarai. Informe técnico de la cuarta campaña de muestreo del 02 al 04 de junio del 2015, 2015.
- Chao X., Jia Y., Shields F.D., Wang S.S., and Cooper C.M. Three-dimensional numerical modeling of cohesive sediment transport and wind wave impact in a shallow oxbow lake. *Advances in Water Resources*, 31(7):1004–1014, 2008.
- Eid B.M. Investigation into interfacial transports and exchange flows for lake models. 1981.
- Facetti J.F. Reflexiones sobre el estado ambiental de la cuenca del Lago Ypacarai. Alternativas de solución. 2007.
- Griebel M., Dornseifer T., and Neunhoffer T. *Numerical simulation in fluid dynamics: a practical introduction*, volume 3. Siam, 1997.
- Issa R.I. Solution of the implicitly discretised fluid flow equations by operator-splitting. *Journal of Computational Physics*, 62(1):40–65, 1986.
- Józsa J. Shallow lake hydrodynamics. Theory, measurement and numerical model applications. *Lecture Notes of the IAHR short course on environmental fluid mechanics, Budapest*, pages 7–16, 2004.
- OpenFOAM. User guide. *OpenFOAM Foundation*, 2(1), 2011.
- Ruíz P.I.R. Recuperación del Lago Ypacarai. 2012.
- SEAM. Mediciones de caudales en el río Salado. url <http://www.seam.gov.py/>, 2015. Consultado el 13-10-2015.
- Tsanis I.K., Wu J., Shen H., and Valeo C. Environmental hydraulics: hydrodynamic and pollutant transport modelling of lakes and coastal waters. *Developments in Water Science*, 56:vii–360, 2006.
- Wu J. Wind-stress coefficients over sea surface near neutral conditions-a revisit. *Journal of Physical Oceanography*, 10(5):727–740, 1980.
- Wu X., Kong F., Chen Y., Qian X., Zhang L., Yu Y., Zhang M., and Xing P. Horizontal distribution and transport processes of bloom-forming microcystis in a large shallow lake (Taihu, China). *Limnologica-Ecology and Management of Inland Waters*, 40(1):8–15, 2010.